Study of Wear Properties of Aluminum Alloy 332 at Difference Sliding Distance

Fizam Zainon [1], Ruslizam Daud [1] & Khairel Rafezi Ahmad [2]
[1] Fracture and Damage Research Group, School of Mechatronic Engineering, Universiti Malaysia Perlis
[2] School of Materials Engineering, Universiti Malaysia Perlis
Email: anna.nocah@gmail.com

Abstract

This paper reports on wear properties of aluminum alloy 332 (AA332) sliding under different distances. A pin on disc wear-testing machine is used to evaluate the wear properties of the AA332, in which a cast iron cylinder block liner is used as the counterface material. The optical microscope equipped with a digital camera is used to analyse the microstructure and worn surfaces of the AA332. The microstructure of AA332 consists of a structure of α-Al matrix, silicon particle and eutectic silicone. The eutectic silicon present as needle-like shape and silicon particle forming as polyhedral or blocky shape. Wear behaviour results show that the volume loss increases proportionally to the sliding distance. The wear coefficient indicated an abrasive wear occurred during sliding and the wear rate also increased with the increase in sliding distance. All the worn surfaces are seen with a distinct pattern of ploughing (grooves and ridges) running parallel to one another ensuring typical characteristic of sliding wear.

Keywords Aluminum Alloy 332, Wear, Pin on Disc, Worn Surface.

1. Introduction

The Al – Si is an ideal material for use in numerous applications because of its low density, low melting temperature, low cost and good mechanical properties (Azmah Hanim et al., 2011; Chung, 2010). Generally, aluminum alloy 332 (AA332) of high thermal conductivity can be used effectively for the manufacturing of pistons (ATZ/MTZ-Fachbuch, 2012), a process that requires the capability of the substance to cope with extreme thermal stress. However, sometimes it cannot meet the requirements of harsh engineering environments such as sliding activities because the wear resistance of AA332 is low. Therefore, the heat treatment is required to improve the wear resistance.

Wear is one of the most universally encountered industrial problems; foremost to the replacement of engineering component (Abouei et al., 2010; Ajith Kumar et al., 2013). Basing on ASTM International G40-13, wear is alteration of a solid surface by a progressive loss of material due to relative motion between that surface and a contacting substance. It's related to the surface damage or removal of material from one or, both of two solid surfaces in sliding, rolling or impact motion relative to one another (Bhushan, 2013) influenced by the applied load, sliding velocity and material characteristics (Corrochano et al., 2011).

Wear includes six primary wear modes, however, the well-known occurred on Al-Si alloy are abrasive and adhesive (Abdi et al., 2013; Bhushan, 2013). Abrasive wear arises when a hard surface or soft surface with hard particles embedded in a surface slide and a ploughing or groove occurred. Meanwhile, adhesive wear known as scoring, galling or seizing, occurs when two

surfaces of slides against each other under pressure. There are two types of adhesive wear namely mild and severe wear (Vijeesh & Narayan, 2014). Mild wear, generally attributed to mechanical mixing and surface oxidation; influenced by the morphology, size and distribution of particles. In mild wear, surface damage becomes less extensive because the load is not sufficient to fracture the particles (Vijeesh & Narayan, 2014) and tribology layers cover the worn surface (Kato & Adachi, 2001). Whereas, severe wear involves massive surface damage and large scale materials flake away or transfer to the counterface. Severe wear occurs mainly due to high loads and high test speeds. Numerous studies have conducted to assess the sliding wear behaviour of Al-Si. However, to understand the role of microstructure, wear and worn surface of AA332 at different sliding distance have been quite limited.

Abouei et al., (2010) study the effect of Fe-rich intermetallics on the wear behaviour of eutectic Al–Si alloy (LM13). The wear rate of the eutectic Al–Si alloy, 1.2Fe (addition of 1.2%Fe to the eutectic Al–Si alloy), 1.2FeMn alloys (addition of Mn to the 1.2Fe alloy) at different applied loads. The authors reported, the 1.2FeMn alloy has the highest wear rate compared to the alloys at all applied loads. This explained based on the microstructural features of the alloys. Authors note, addition of iron (Fe) to the eutectic Al–Si alloy led to the precipitation β-phase intermetallic (β-Al_5FeSi) in the matrix. As knew the β-Al_5FeSi intermetallics are hard and brittle phase; exist as separated the particles by a highly faceted nature in the alloy matrix. Meanwhile, the addition of Mn to the 1.2Fe alloy damaging the effect of iron on replacement of β-flake-like intermetallics to α-intermetallic compounds and enhanced the wear resistance of the 1.2FeMn alloy. Authors have reported the worn surface of the alloys under applied loads of 18 and 100 N. The worn surface under functional load of 18 N was covering with oxide particles. The oxide particles formed on the overall worn surface of the pin contained a certain amount of iron, aluminum and oxygen. The debris entrapped between the sliding surfaces and compacted due to the repetitive sliding; forms a tribolayer over the surface.

Ajith Kumar et al., (2013) investigate the dry sliding wear behaviour of pure Mg, hypoeutectic and hypereutectic Mg–Si alloys prepared using the gravity casting method. The authors reported the wear resistance of hypereutectic Mg–Si alloys is greater than hypoeutectic alloys; due to the morphology of the primary Mg_2Si change from polyhedral to coarse dendrite. Moreover, the presence of the lamellar Mg_2Si and soft dendrites α - Mg in the hypoeutectic alloys also contributed a higher wear resistance. Meanwhile, the worn surface of the both alloy shows a distinct pattern of grooves and ridges running parallel with one another; ensuring typical characteristic of sliding wear. All tested samples appeared as deep scratches; base on the hard asperities of counter face or detached particles that are removed from the pin and placed on the contact surface.

Feyzullahoglu & Sakiroglu, (2011) study the tribology behaviours of aluminum based materials under dry sliding. Four different aluminum alloys are produced by casting and tested on a pin on disc wear testing machine. One of the alloys is $Al_{8.5}Si_{3.5}Cu$; produced in the induction furnace at 800°C and cast into a cylindrical metal die. Results of $Al_{8.5}Si_{3.5}Cu$ alloy shows better wear resistance and least wear loss compared to other alloys. The authors noted that the hardness and hard Si phase of $Al_{8.5}Si_{3.5}Cu$ alloy provides an excellent wear resistance for this alloy. As it known, the wear behaviours under dry sliding conditions are determined by material properties like strength, hardness, and internal structure. In addition, Si particulates covered by ductile and firm aluminum matrix increase the toughness of the material and provide resistance towards wearing by preventing plastic deformation.

The proposed and novelty of this study is a discussion on microstructure, wear behaviours and worn surface of the AA332 alloy at different sliding distance.

2. Experimental Procedure

Chemical composition of the alloy was analyzed using Optical Emission Spectrometer (Q8 MAGELLAN) metal analysis tester and Energy Dispersive X-ray Spectroscopy (EDX) tester. The density was measured using Gas Pycnometer Micromeritics AccuPyc ll 1340 tester. The morphology and the worm surface of the alloy was observed using an optical microscope (Olympus, BX41M) equipped with a digital camera (PowerShot A460) and the image was analysis using Image J software. Hardness analysis was performed by using Vicker's hardness tester (model FV-700e) following ASTM International E384-11.

Dry wear tests of the specimens were performed using a pin on a disc sliding wear testing machine; modified from Metkon Gropo 1V grinder-polishing, as outlined in the protocol of ASTM International G99-05. The test samples were clamped into a vertical sample holder and against a cylinder block liner. The block liner is a grey cast iron material with a hardness of Hv 266.4. The test samples with the dimensions of 10 mm (diameter) x 10 mm (height) were contact with the block liner, which had an external diameter of 63 mm.

The test was conducted at a load of 10 N, a constant sliding speed of 1.0 m/s and a sliding distance of 100, 250, 500, 1000 and 2000 m. Before each test, the samples and the block liner cleaned with acetone and dried with the clean cloth. The surfaces of the test sample and block liner and were finished with 600-grit SiC abrasive paper. An electronic weight balance with an accuracy of 0.1 mg used to measure the weight of the samples before and after each test. The detailed wear apparatus is illustrated in Fig. 1.

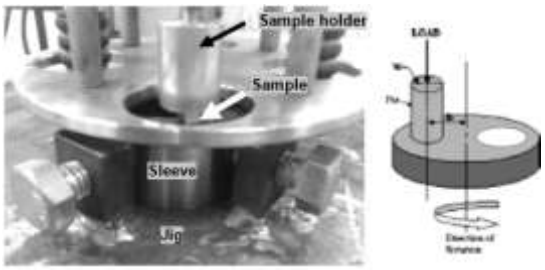

Figure 1 Wear apparatus and diagram of pin on disc

The volume loss (V) was determined using equation 1, wear coefficient (k) was using equation 2 (Ajith Kumar et al., 2013) and wear rate (Q) was calculated using volume loss per sliding distance (mm^3/m) as Archard's equation (Eq. 3) (Abdi et al., 2013).

$$V = \Delta W/\varrho \quad (1)$$

$$K = (3VH_v)/FS \quad (2)$$

$$Q = (KFS)/H_v \quad (3)$$

where, V is volume loss (mm^3), ΔW is weight loss (g) and ϱ is density (g/mm^3), k is wear coefficient, Hv is hardness - Vickers scale (kg/mm^2), F is load (kg), S is sliding distance (mm) and Q is wear rate (mm^3/m).

3. Results and Discussion

Table 1 shows the chemical compositions and mechanical properties of AA 332. The silicon composition of AA332 has recorded 11 wt% follow by other elements as usually contained in Al-Si alloy.

Table 1 Chemical Composition and properties of AA332

	Element (wt%)										*Hardness*	*Density*
	Si	*Fe*	*Cu*	*Mn*	*Mg*	*Ni*	*Zn*	*Ti*	*Other*	*Al*	*Hv*	*(g/cm3)*
AA332	*11*	*0.9*	*1.6*	*0.2*	*0.3*	*0.1*	*1.0*	*0.1*	*0.2*	*rest*	*95.36*	*2.89*

Generally, the composition of AA332 contains two types of alloying elements there are silicon and copper. The content of silicon in the Al–Si alloys varies from 4 to 25 wt% of silicon, where it classified as hypoeutectic (< 12 wt% Si), eutectic (12 – 13 wt% Si) and hypereutectic (14 – 25 % Si) (Vijeesh & Narayan, 2014). Meanwhile Panwar & Pandey, (2013) and Zhang et al., (2012) mentioned the composition with 11 wt% of Si is hypoeutectic alloy but near to the eutectic composition.

The silicon content of this alloy provides fluidity and castability better than to those of other materials. (Azmah Hanim et al., 2011) noted that, the fluidity refers to the ability of the liquid metal to flow through a mould without prematurely solidifying and castability refers to the ease with which a suitable casting can be made from the alloy. Other elements are present to obtain improvement in the AA332 such as lowering the thermal expansion coefficient, increasing the high-temperature strength and increase the abrasion resistance.

3.1 Microstructural Analysis

Optical photomicrograph of AA332 alloy presented in Fig. 2. As it is observed in Fig. 2(a), dendritic of α-Al matrix forming as equiaxed grain and it is dominated in the microstructure of the alloy. While, Fig. 2(b - c) shows the microstructure consists of a structure of α-Al matrix, silicon particle and eutectic silicon and all samples show free from porosity. In Fig. 2(b), eutectic silicon particles present as needle-like shape; continues along the α-Al matrix grain boundaries and in Fig. 2(c) show the silicon particle forming as polyhedral or blocky shape.

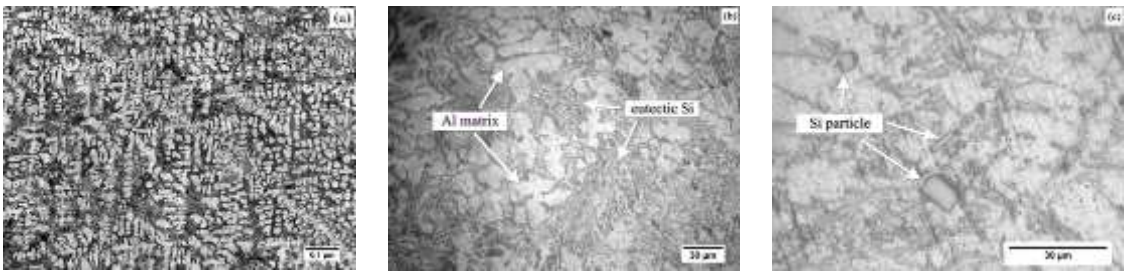

Figure 2 Optical micrograph of AA332

As it is known, when Al–Si alloy solidifies, the primary aluminum forms and grows as dendrites, whereas silicon solidifies formed as silicon phase. As mentioned by Zeren, (2007), Al-Si alloys contain with two kinds of silicon phase (i) plate-like eutectic silicon and (ii) coarse primary silicon particle. The microstructure of plate-like eutectic silicon particles commonly found in unmodified hypereutectic alloy can be forming as needle-like or spheroidization shape.

Eutectic silicon particles play a significant character in determining the mechanical properties; the size and morphology of the eutectic silicon particles are basically responsible for the improved or deteriorated mechanical properties of an Al-Si alloy (Hany Ammar, 2010).

Plate-like particles forming from primary silicon particles nucleate and grow isotropically under low cooling rates (Vijeesh & Narayan, 2014). The size and morphology of silicon particles results in enhanced ductility and strength, ultimately having the effect of improved quality. Meanwhile, Vijeesh & Narayan, (2014) pointed, the presence of coarse primary silicon has a destructive effect on the extrudability, machinability, strength and ductility of the alloy; meanwhile, the fine primary silicon particles are desirable for better mechanical properties and wear resistance.

3.2 Wear Behaviour

An accelerated loss of material from the operating surfaces as a result of relative motion is commonly referred to as wear. The wear properties of the Al-Si alloy are considerably dependent on the morphology, size and distribution of the primary silicon (Vijeesh & Narayan, 2014). The wear properties and sliding distance relationship in dry sliding condition are shown in Fig. 3. Clearly seen in Fig. 3(a), the volume loss has increased slowly from initial until up to 500 meters, then increase rapidly until 2000 meters. Experimental suggested the volume loss increases with the sliding distance at constant velocity. As mentioned by Feyzullahoglu & Sakiroglu, (2011), in dry sliding state, the volume loss occurs as a result of wear increases normally with sliding distance. This is because as a sliding distance increases, the temperature will rise and there is a tendency for soft surface penetration by the harder asperities. Moreover, the particle easy removed from the surface because of the silicon structure. As shown in Fig. 2(b), the eutectic silicon particles present as needle-like shape; continues along the α-Al matrix grain boundaries. Vijeesh & Narayan, (2014) agreed the network of needle-like eutectic silicon in non-heat treated Al-Si is less connected to each other; where fracture or crack easily occurs.

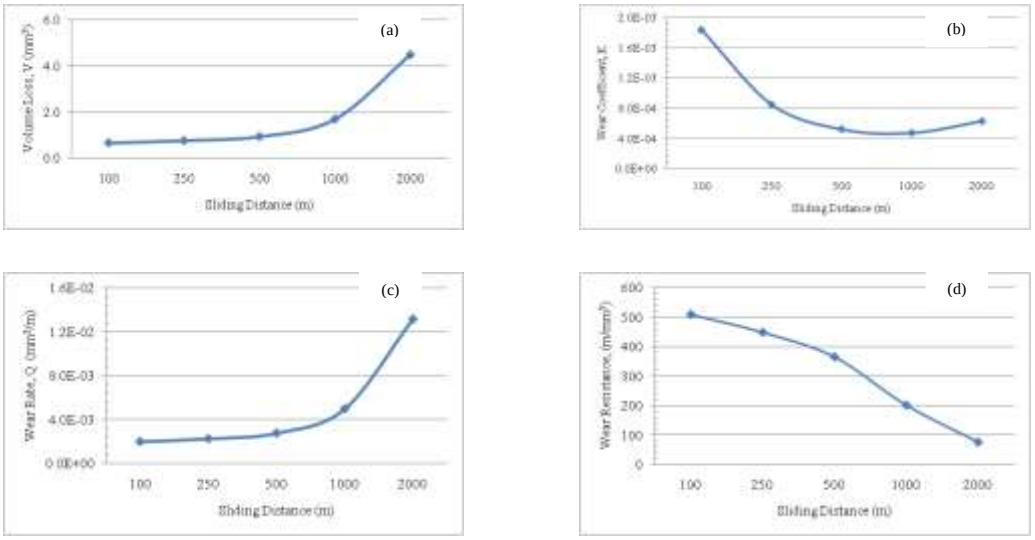

Figure 3 Wear properties of AA332 (a) volume loss (b) wear coefficient (c) wear rate (d) wear resistance

Based on the results has recorded in Fig. 3(b), the abrasive wear has occurred during dry sliding test. This is explained by the fact that the ranges of wear coefficient (k) of AA332 show among 10^{-}

^{4} to 10^{-3}. As noted by Bhushan, (2013) and Kato & Adachi, (2001), the value of k for abrasive wear are from 10^{-6} to 10^{-1}. Furthermore, the evidence of the abrasive wear can also be seen in worn surface analysis. All the worn surfaces are seen with the distinct pattern of grooves and ridges running parallel to sliding direction.

Wear process is generally quantified by wear rate. Wear rate is defined as the volume or mass of material removed per unit time or per unit sliding distance (Ajith Kumar et al., 2013; Bhushan, 2013). As showed in Fig. 3(c), the wear rate of the AA332 increases sharply with increases in sliding distance from $1.97X10^{-3}$ to $1.32\ X10^{-2}$ mm^3/m. As per Archard's relation, wear rate increases in sliding, related to asperity-to-asperity contact (Kathiresan & Sornakumar, 2010). Refer to Fig. 3(c), the stages of run-in period start from initial sliding until 250 meters. During this condition, the wear rate remains constant and may change if the transition from one mechanism to another occurs during a test. Wear rate during run-in period depends on the material structure, properties and surface conditions such as surface finish and the nature of any films present (Bhushan, 2013).

The steady-state sliding region has been covered between sliding at 500 to 2000 meters. During this region, the surface roughness is replaced by plastic deformation. Clearly seen, material removal from plastic deformation during a test occurred by ploughing (groove and ridge). The ploughing process can cause the subsurface plastic deformation and contribute to the nucleation of surface and subsurface cracks or fracture. Meanwhile, Kato & Adachi, (2001) noted that, the large plastic deformation in the region sometimes forms a wedge-like shape, which is accompanied by crack initiation and propagation in the combined fracture mode of tensile and shear. The wear rate and surface damage can be minimised if the plastic deformation of the material at the contact interface is prevented.

Wear resistance of AA332 alloys with respect to the sliding distance is shown in Fig. 3(d). The wear resistance show declined from $5.09X10^{2}$ to $7.58X10^{1}$ m/mm^3 during sliding among 100 to 2000 meters; it is diminished 85% from the initial rate. The worst wear resistance recorded for AA332 can be attributed to the present of needle-like eutectic silicon. (Vijeesh & Narayan, 2014) agreed the wear resistance of the unrefined alloy affected due to the poor bonding between the α aluminum and needle-like eutectic silicon. The authors noted that, the sharp corners of the needle-like eutectic silicon act as a stress raiser in initiation and propagation of the crack or fracture through the aluminum matrix (Vijeesh & Narayan, 2014).

3.3 Worn Surface

Topographical studies of the worn surfaces of the material can present a superior platform to understand the wear mechanism of the material. Optical micrograph was done on the worn surfaces of the AA332 tested at 10 N loads are depicted in Fig. 4. All the worn surfaces are seen with a distinct pattern of ploughing (grooves and ridges) running parallel to one another ensuring typical characteristic of sliding wear. Ploughing as a result of the plastic flow of the softer material against a harder surface. In the ploughing process, material is displaced from a groove to the sides without the removal of material

Light ploughing and no obvious deep groove are observed in Fig. 4(a) and confirmed that the abrasive wear occurred during sliding. Bhushan, (2013) agreed, in most abrasive wear situations, scratching (of mostly the softer surface) is found to be a series of grooves parallel to the direction of sliding (ploughing).

Fig. 4(b) shows a deep and wide groove along with small delaminations is observed on the worn surfaces. It may be attributed by the hard asperities of counter face or detached particles

that are removed from the pin and placed on the contact surface. Under severe sliding condition, gross plastic deformation occurs on the surface and the material is extruded from the interface before re-solidifying around the pin periphery (Ajith Kumar et al., 2013). It can be seen a delamination is observed on the surface due to flow of materials along the sliding direction.

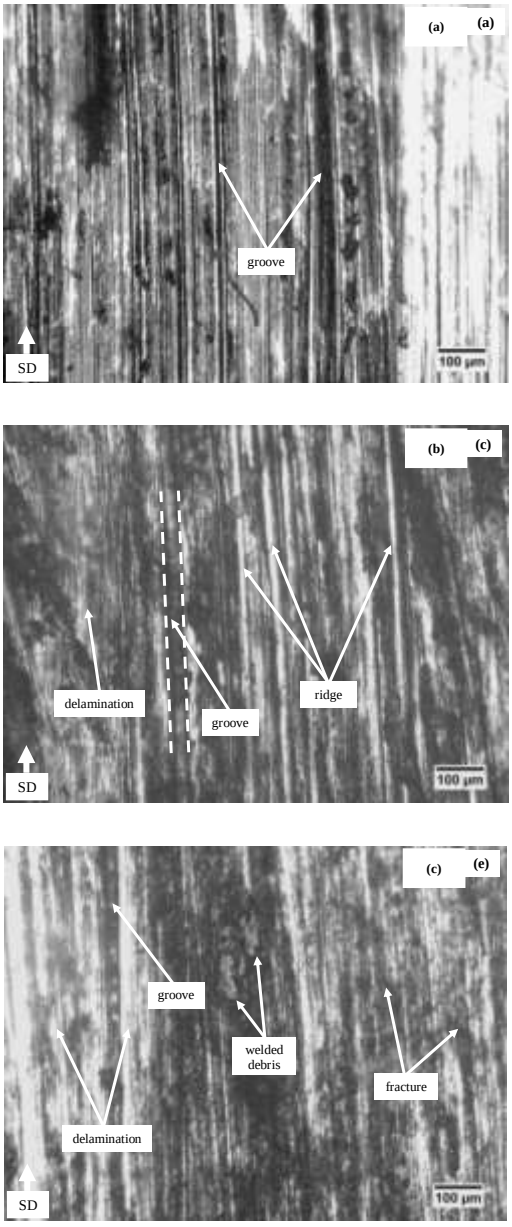

Figure 4 Optical micrograph of worn surface tested at 10 N load with variation of sliding distance (a) 100 meters (b) 500 meters (c) 2000 meters

Delamination is a fatigue-related wear mechanism, repeated sliding induces subsurface cracks on the wear surface that gradually grow and eventually shear to the surface. Panwar & Pandey, (2013) noted that, micro cracks are the main source of delamination or remove the material during the wear test.

A wide delaminations, welded debris and fracture on the surface are observed in Fig. 4(c). Fracture occurred when ridges of the ploughed grooves become flattened owing to sliding for several times and material was removal by a low-cycle fatigue mechanism. During sliding contact, the fracture of particles may arise from either strain transfer from surrounding plastically

deforming matrix alloy (Wilson & Alpas, 1997). Moreover, abrasive grooving with the hard and sharp asperity is possible fractured by sliding (Kato & Adachi, 2001). The authors pointed out that, in a brittle material, which is indented and ploughing by the abrasive, a wear particle is generated due to mainly brittle fractures caused by initiation and propagation of cracks.

4. Conclusions

The main conclusions drawn from the present work are as follows:

i. The chemical composition of AA332 contains 11 wt% of Si. It is hypoeutectic alloy but near to the eutectic composition and suitable for casting process.
ii. The eutectic silicon present as needle-like shape and silicon particle forming as polyhedral or blocky shape. The presence of needle-like eutectic silicon contributes a poor wear resistance for AA332. Therefore, heat treatment is suggested to modify the eutectic silicon structure from needle-like to spheroidization shape.
iii. The k value (wear coefficient) indicated an abrasive wear occurred during sliding. It has recorded between 10-4 to 10-3.
iv. The wear rate increased with increases in sliding distance; related to asperity-to-asperity contact.
v. The wear resistance show declined during sliding from 100 to 2000 meters; it is reduced 85% from the initial rate.
vi. All the worn surfaces are seen with a distinct pattern of ploughing running parallel to the slide path. Groove, ridge, delamination and fracture are observed on the worn surface.

Acknowledgement

The author would like to thank Universiti Malaysia Perlis, Dr Khairel Rafezi Ahmad and Dr Ruslizam Daud for their kind assistance in this research.

References

Abdi, M., Taheri, A. K., & Bakhtiarydavijani, A. (2013). A New Analysis Method of the Dry Sliding Wear Process Based on the Low Cycle Fatigue Theory and the Finite Element Method. *Journal of Materials Engineering and Performance*, *23*(3), 1096–1106.

Abouei, V., Saghafian, H., Shabestari, S. G., & Zarghami, M. (2010). Effect of Fe-rich Intermetallics on the Wear Behavior of Eutectic Al–Si Piston Alloy (LM13). *Materials & Design*, *31*(7), 3518–3524.

Ajith Kumar, K. K., Pillai, U. T. S., Pai, B. C., & Chakraborty, M. (2013). Dry Sliding Wear Behaviour of Mg–Si Alloys. *Wear*, *303*(1-2), 56–64.

ASTM International E384-11. (2011). *Standard Test Method for Knoop and Vickers Hardness of Materials.* In *ASTM Book of Standards*. Philadelphia, USA: American Society for Testing and Materials.

ASTM International G40-13. (2014). *Standard Terminology Relating to Wear and Erosion*. In *ASTM Book of Standards*. Philadelphia, USA: American Society for Testing and Materials.

ASTM International G99-05. (2010). *Standard Test Method for Wear Testing with a Pin-on-Disk Apparatus*. In *ASTM Book of Standards*. Philadelphia, USA: American Society for Testing and Materials.

ATZ/MTZ-Fachbuch. (2012). *Pistons Materials*. In G. MAHLE (Ed.), *Piston and Engine Testing*. Stuttgart: Springer Fachmedien Wiesbaden GmbH.

Azmah Hanim, Chung, S. C., & Chuan, O. K. (2011). Effect of a Two-Step Solution Heat Treatment on the Microstructure and Mechanical Properties of 332 Aluminium Silicon Cast Alloy. *Materials & Design*, *32*(4), 2334–2338.

Bhushan, B. (2013). *Introduction To Tribology* (Second Ed.). New York, USA: John Wiley & Sons, Inc.

Chung, D. D. L. (2010). *Composite Materials. Science and Applications*. (Second Ed.). London: Springer-Verlag London.

Corrochano, J., Lieblich, M., & Ibanez, J. (2011). The Effect of Ball Milling on the Microstructure of Powder Metallurgy Aluminium Matrix Composites Reinforced with $MoSi_2$ Intermetallic Particles. *Composites Part A*, *42*(9), 1093–1099.

Feyzullahoglu, E., & Sakiroglu, N. (2011). The Tribological Behaviours of Aluminium-Based Materials Under Dry Sliding. *Industrial Lubrication and Tribology*, *63*(5), 350–358.

Hany Ammar. (2010). *Influence of Metallurgical Parameters on the Mechanical Properties and Quality Indices of Al-Si-Cu-Mg and Al-Si-Mg Casting Alloys*. University of Quebec At Chicoutimi.

Kathiresan, M., & Sornakumar, T. (2010). Friction and Wear Studies of Die Cast Aluminum Alloy-Aluminum Oxide-Reinforced Composites. *Industrial Lubrication and Tribology*, *62*(6), 361–371.

Kato, K., & Adachi, K. (2001). *Wear Mechanisms*. In B. Bhushan (Ed.), *Modern Tribology Handbook. Vol 1* (First Ed.). Washington D.C: CRC Press.

Panwar, R. S., & Pandey, O. P. (2013). Analysis of Wear Track and Debris of Stir Cast LM13/Zr Composite at ElevatedTtemperatures. *Materials Characterization*, *75*, 200–213.

Vijeesh, V., & Narayan, P. K. (2014). Review of Microstructure Evolution in Hypereutectic Al–Si Alloys and its Effect on Wear Properties. *Transactions of the Indian Institute of Metals*, *67*(1), 1–18.

Wilson, S., & Alpas, A. T. (1997). Wear Mechanism Maps for Metal Matrix Composites. *Wear*, *212*(1), 41–49.

Zeren, M. (2007). The Effect of Heat Treatment on Aluminum Based-Piston Alloys. *Materials & Design*, *28*, 2511–2517.

Zhang, L., Eskin, D. G., Miroux, A., & Katgerman, L. (2012). *Formation of Microstructure in Al-Si Alloys Under Ultrasonic Melt Treatment*. In C. E. Suarez (Ed.), *Light Metals 2012*. USA: TMS (The Minerals, Metals & Materials Society).